Biological Psychiatry

Archival Report

Metabotropic Glutamate Receptor 5 in Amygdala Target Neurons Regulates Susceptibility to Chronic Social Stress

Jeongseop Kim, Shinwoo Kang, Tae-Yong Choi, Keun-A Chang, and Ja Wook Koo

ABSTRACT

BACKGROUND: Metabotropic glutamate receptor 5 (mGluR5) has been implicated in stress-related psychiatric disorders, particularly major depressive disorder. Although growing evidence supports the proresilient role of mGluR5 in corticolimbic circuitry in the depressive-like behaviors following chronic stress exposure, the underlying neural mechanisms, including circuits and molecules, remain unknown.

METHODS: We measured the c-Fos expression and probability of neurotransmitter release in and from basolateral amygdala (BLA) neurons projecting to the medial prefrontal cortex (mPFC) and to the ventral hippocampus (vHPC) after chronic social defeat stress. The role of BLA projections in depressive-like behaviors was assessed using optogenetic manipulations, and the underlying molecular mechanisms of mGluR5 and downstream signaling were investigated by Western blotting, viral-mediated gene transfer, and pharmacological manipulations.

RESULTS: Chronic social defeat stress disrupted neural activity and glutamatergic transmission in both BLA projections. Optogenetic activation of BLA projections reversed the detrimental effects of chronic social defeat stress on depressive-like behaviors and mGluR5 expression in the mPFC and vHPC. Conversely, inhibition of BLA projections of mice undergoing subthreshold social defeat stress induced a susceptible phenotype and mGluR5 reduction. These two BLA circuits appeared to act in an independent way. We demonstrate that mGluR5 overexpression in the mPFC or vHPC was proresilient while the mGluR5 knockdown was prosusceptible and that the proresilient effects of mGluR5 are mediated through distinctive downstream signaling pathways in the mPFC and vHPC.

CONCLUSIONS: These findings identify mGluR5 in the mPFC and vHPC that receive BLA inputs as a critical mediator of stress resilience, highlighting circuit-specific signaling for depressive-like behaviors.

https://doi.org/10.1016/j.biopsych.2022.01.006

More than 300 million people worldwide, i.e., approximately 4.4% of the world's population, are estimated to have depression (1). Accumulating evidence suggests that stressful life events can increase the risk of developing depression (2,3). However, not all stress-exposed individuals develop stress-related psychiatric disorders, such as major depressive disorder, and some individuals are vulnerable to stress, while others maintain normal psychophysiological functioning (4,5).

It has been reported that the glutamatergic system in brain regions such as the basolateral amygdala (BLA), medial prefrontal cortex (mPFC), and hippocampus (HPC) plays a critical role in both stress susceptibility and resilience (6–8). The BLA is involved in emotional valence processing, both positive and negative (9,10). Recent studies have shown that distinct BLA cell populations are responsible for fear-, anxiety-, and/or depression-related behaviors via unique long-range projections to brain regions such as the mPFC and ventral HPC (vHPC) (11–15). Deficits of the glutamate neurotransmitter system in these brain areas have been reported to be associated with chronic stress and depression (16,17).

In particular, dysfunctional metabotropic glutamate receptor 5 (mGluR5) signaling has been implicated in the pathophysiology of stress-related psychiatric disorders (18,19). Despite some inconsistencies (20,21), a large amount of evidence supports the proresilient role of mGluR5 in patients with depression. Previous neuroimaging studies have reported decreased mGluR5 binding or glutamate metabolites in the PFC and HPC of subjects with depression (18,19,22). Reduced mGluR5 expression was also observed in the postmortem PFC of patients with major depressive disorder (23). Genome-wide association studies and meta-analyses have also revealed reduced *Grm5* (encoding mGluR5) expression (24) in patients with major depressive disorder. Preclinical studies have shown that chronic corticosterone and stress downregulate mGluR5 expression and density in some brain regions, including the HPC (25–27). Consistently, mGluR5 knockout, particularly in PFC glutamatergic neurons, promotes depressive-like behaviors (28,29).

SEE COMMENTARY ON PAGE 98

 ISSN: 0006-3223

Despite this evidence for a proresilient role of mGluR5, the underlying neural mechanisms, including circuits and molecules, are largely unknown in the context of chronic stress. In this study, we investigated a presynaptic activity–dependent role of postsynaptic mGluR5 in molecular and behavioral responses to chronic social defeat stress (CSDS) in an ethologically validated animal model of depression (30,31), with a focus on projections from the BLA to the mPFC (BLA→mPFC) or the vHPC (BLA→vHPC). Our results demonstrate that activation of BLA projections and activity-dependent mGluR5 signaling in the mPFC and vHPC affect depressive-like behaviors.

METHODS AND MATERIALS

Animals

Eight-week-old male C57BL/6NCrljOri mice (25–30 g; Orient Bio) and 3- to 8-month-old male CrlOri: CD-1 (35–45 g; Orient Bio) were used. Food and water were provided ad libitum during the acclimation period to the polycarbonate cage under a 12-hour light/dark cycle. The temperature and humidity of the breeding room were maintained at 22 ± 2 °C and 50 ± 10%. All experimental procedures followed the Korea Brain Research Institute guidelines and Institutional Animal Care and Use Committee (M1-IACUC-19-0009).

Stress Exposure and Behavior Test for Depressive-like Behaviors

CSDS and subthreshold social defeat stress (SSDS) were conducted as described previously (32–34). For CSDS, each C57BL/6N mouse was exposed to 10 minutes of physical aggression by a CD-1 mouse. After the session, the defeated C57BL/6N mice were housed overnight within the same cage as the CD-1 mice on the opposite side of a transparent and perforated divider to provide sensory, but not physical, contact. The procedure was repeated for 10 consecutive days with a new aggressor on each day. For SSDS, mice were exposed to three social defeat sessions with 5 minutes of physical defeat followed by 15 minutes with no defeat. All stressed mice received the social interaction test 24 hours after the last defeat episodes and the sucrose preference test.

Viral Injection

Stereotaxic surgeries of viral injections were performed for the retrograde mapping of BLA→mPFC or BLA→vHPC projection neurons (PNs), ex vivo electrophysiological experiments, repeated optical activation/inactivation of BLA→mPFC and/or BLA→vHPC PNs, and localized *Grm5* gene overexpression or knockdown.

Cannula Implantation and Microinfusions

Animals received bilateral intra-mPFC or -vHPC infusions of 10 mM LY294002 [PI3K/Akt (phosphatidylinositol 3-kinase/Akt) inhibitor, 1 μg/0.25 μL/side] or 2 mM U0126 [MAPK/ERK (mitogen-activated protein kinase/extracellular signal–regulated kinase) inhibitor, 1 μg/0.25 μL/side] at a continuous rate of 0.1 μL/min via a microinfusion pump (Legato 200; KD Scientific) around 15 minutes before SSDS.

Ex Vivo Electrophysiology

To assess the paired-pulse ratio (PPR) of excitatory or inhibitory postsynaptic currents and AMPA/NMDA ratio, whole-cell patch-clamp recordings were obtained from pyramidal neurons of the mPFC or vHPC in acute brain slices from mice that had been stereotaxically injected with AAV5–Syn-ChrimsonR-tdTomato into the BLA.

Data Analysis

We confirmed normality (Shapiro-Wilk test) and equal variance (Bartlett's test) on all data before a parametric analysis unless otherwise indicated. To assess differences between the two experimental groups, Student's *t* tests, Student's *t* tests with Welch's correction (for datasets with unequal variances), and Mann-Whitney *U* tests (for non-normally distributed data) were used. For the analysis of three or more groups, one-way analysis of variance (ANOVA) with Tukey's post hoc tests or with Welch's post hoc tests (for data sets with unequal variances) and the Kruskal-Wallis *H* test with Dunn's post hoc tests (for non-normally distributed data) were used. To analyze CSDS effects on the topographical distribution of activated BLA projections, two-way ANOVAs with Fisher's protected least significant difference post hoc tests were used. For details, see Supplemental Methods in Supplement 1 and Table S2 in Supplement 2.

Additional Details

See Supplemental Methods in Supplement 1 for additional routine procedures and information, including immunofluorescence, real-time quantitative polymerase chain reaction, and Western immunoblot analysis.

RESULTS

CSDS Reduces Cell Activity in BLA PNs

We investigated whether expression of c-Fos or other immediate early genes, such as activity-regulated cytoskeleton-associated protein (ARC) and early growth response 1 (EGR1), can be used as readouts for neural activity in BLA neurons projecting to the mPFC (BLA→mPFC) or vHPC (BLA→vHPC). Two weeks after injection of AAVrg-hsyn-ChR2-EYFP or AAVrg-hsyn-Jaws-KGC-GFP-ER2 into the mPFC or vHPC (Figures S1A and S2A in Supplement 1), each mouse received 5 minutes of photostimulation or photoinhibition over BLA PNs for a single day or 10 consecutive days without defeat stress exposure. A single-day 5-minute optogenetic acute activation, but not acute inhibition, altered the expression of c-Fos, ARC, and EGR1 at 90 minutes after optogenetic manipulation (Figure S1B–H in Supplement 1). However, we could not observe acute optogenetic effects 24 hours after acute photomanipulation (Figure S1I–O in Supplement 1). As a result of a once-daily 5-minute optogenetic activation over BLA PNs for 10 consecutive days, we observed that c-Fos expression was increased both at 90 minutes (Figure S2B–H in Supplement 1) and 24 hours after the last optic manipulation compared with the control group (Figure S2I–O in Supplement 1). In contrast, 10-day photoinhibition of BLA PNs decreased c-Fos expression at both time points. However, these chronic optogenetic effects were not explicit for ARC and EGR1 expression. These

observations support the use of c-Fos as an appropriate readout that reflects the rise and fall of chronic neural activity in both BLA→mPFC and BLA→vHPC PNs.

We then investigated whether CSDS affects the activation of BLA→mPFC or BLA→vHPC PNs. We injected AAVrg-hSyn-EGFP into the mPFC and AAVrg-hSyn-mCherry into the vHPC (Figure 1A). After 2 weeks of recovery, the mice received 10 days of CSDS. The social interaction ratio was assessed in a social interaction test that proceeded 24 hours after the last defeat. Animals were sacrificed 90 minutes after the behavioral tests for c-Fos immunolabeling, as described in previous studies (35,36). After triple-immunofluorescence labeling, BLA tissues were imaged in at 4 to 6 anterior-posterior (AP) coordinates and retrogradely labeled BLA PNs were counted (Figure S3A in Supplement 1). BLA→mPFC PNs [EGFP+ (green)/DAPI+] were present throughout the entire

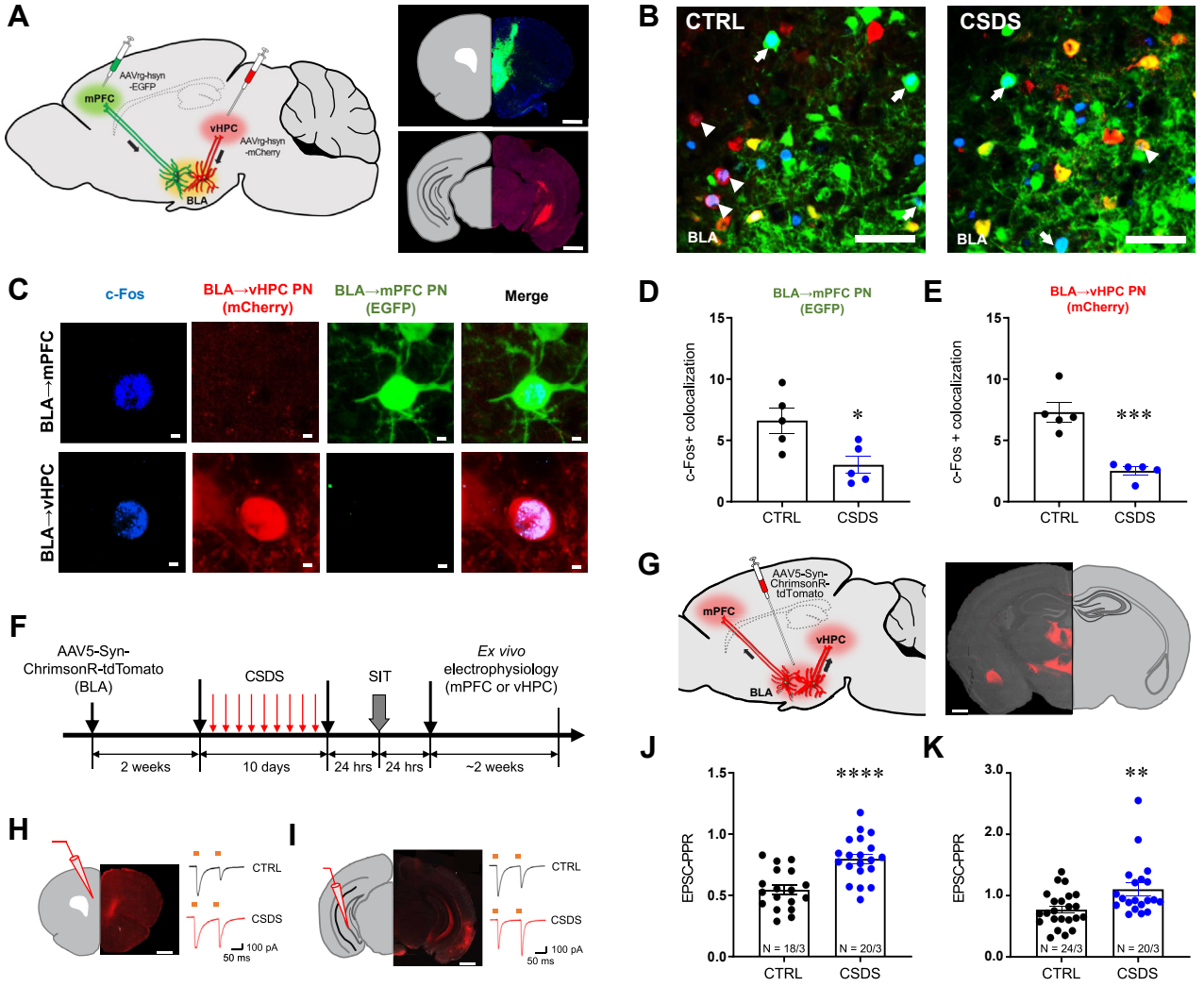

Figure 1. CSDS effects on cell activation and synaptic function in BLA neurons projecting to the mPFC or vHPC. **(A)** Schematic of AAVrg-hSyn-EGFP injection into the mPFC and AAVrg-hSyn-mCherry into the vHPC, and confocal images showing injection sites. Scale bars = 1 mm. **(B, C)** Representative confocal images show c-Fos+ (blue), BLA→mPFC PNs (green), and BLA→vHPC PNs (red) in the BLA. Scale bars = 50 μm **(B)** and 5 μm **(C)**. **(D, E)** c-Fos+ BLA→mPFC PNs (blue + green, arrows in panel **(B)**, unpaired *t* test, $t_8 = 2.896$, $p = .0200$, $n = 5$) or c-Fos+ BLA→vHPC PNs (blue + red, arrowheads in B, unpaired *t* test, $t_8 = 5.661$, $p = .0005$, $n = 5$) were decreased in the intermediate part of the BLA (−1.5 to −1.7 mm AP from the bregma) in CSDS compared with CTRL mice. For CSDS effects on distribution of c-Fos+ BLA PNs at the anterior (−1.1 to −1.3 mm AP) or posterior (−1.9 to −2.1 mm AP) BLA, see Figure S1H and I in Supplement 1. **(F, G)** Experimental procedures for ex vivo electrophysiology using AAV5-Syn-ChrimsonR-tdTomato infusion into the BLA (−1.6 mm AP). Scale bar = 1 mm. **(H, I)** Representative EPSC-PPR evoked by photostimulation of axon terminals from the BLA into the mPFC **(H)** and vHPC **(I)**. Red squares indicate light pulse delivery. Scale bars = 1 mm. **(J, K)** EPSC-PPR was increased in BLA→mPFC synapses **(J)** (unpaired *t* test, $t_{17} = 4.508$, $p = .0003$, $n = 18, 20$) and in BLA→vHPC synapses **(K)** (Welch's *t* test, $t_{31.45} = 2.816$, $p = .0083$, $n = 23, 20$) of CSDS mice. Student *t* test (unpaired), $^*p < .05$, $^{**}p < .01$, $^{***}p < .001$, $^{****}p < .0001$. Data represented as mean ± SEM. AP, anterior-posterior; BLA, basolateral amygdala; CSDS, chronic social defeat stress; CTRL, control; EGFP, enhanced green fluorescent protein; EPSC, excitatory postsynaptic current; mPFC, medial prefrontal cortex; PN, projection neuron; PPR, paired-pulse ratio; SIT, social interaction test; vHPC, ventral hippocampus.

BLA with a highest density at approximately −1.6 mm AP from bregma. Conversely, BLA→vHPC PNs [mCherry+ (red)/DAPI+] were preferentially located in the posterior part of the BLA (sparse around −1.0 mm AP from bregma and reaching a plateau around −1.6 mm AP), but with a smaller density across the entire BLA than BLA→mPFC PNs (Figure 1B, C; Figure S3B in Supplement 1).

Our retrograde localization and further analyses showed that CSDS had no effect on the relative cell numbers of BLA→mPFC (EGFP+/DAPI+) PNs, BLA→vHPC (mCherry+/DAPI+) PNs, or co-projection BLA neurons (EGFP+/mCherry+/DAPI+) in the anterior (−1.1 to −1.3 mm AP), intermediate (−1.5 to −1.7 mm AP), or posterior sections (−1.9 to −2.1 mm AP) of the BLA (Figure S3C–F in Supplement 1). Most importantly, despite null effect of CSDS on the overall number of c-Fos+ cells [c-Fos+ (white)/DAPI+] (Figure S1G in Supplement 1), the number of c-Fos+ cells that were colocalized in the BLA→mPFC (c-Fos+/EGFP+/DAPI+) and/or BLA→vHPC (c-Fos+/mCherry+/DAPI+) circuits were decreased by CSDS compared with that in control mice (Figure 1D, E; Figure S3H, I in Supplement 1). These data suggest that CSDS effects on cell activity are circuit specific in the BLA. In addition, we observed that both BLA→mPFC or BLA→vHPC PNs were mostly colabeled with CamKIIα+, a glutamatergic marker (∼80%), but not with GAD67+, a GABAergic (gamma-aminobutyric acidergic) marker (1%–2%). These data indicate that BLA PNs are mostly excitatory glutamatergic neurons, rarely inhibitory GABAergic neurons, as shown in previous studies (37,38) (Figure S4 in Supplement 1). Taken together, these data suggest that CSDS may reduce the excitatory activity of BLA→mPFC or BLA→vHPC PNs.

We directly assessed the effects of CSDS on circuit-specific glutamatergic synaptic transmission from the BLA using ex vivo optogenetic patch-clamp electrophysiology. Two weeks after we injected AAV5-Syn-ChrimsonR-tdTomato into the BLA, the mice were exposed to CSDS for 10 days (Figure 1F, G; Figure S5A in Supplement 1). Then, synaptic transmissions were recorded in mPFC or vHPC neurons by activating ChrimsonR-expressing axon terminals from the BLA (Figure 1H, I; Figure S5B in Supplement 1). We found that CSDS significantly increased the PPRs of the excitatory postsynaptic current in both BLA→mPFC (Figure 1J) and BLA→vHPC (Figure 1K) synapses. However, the inhibitory postsynaptic current PPRs and AMPA/NMDA ratios were not altered (Figure S5B–F in Supplement 1). These results suggest that CSDS decreases glutamate release probability (39,40) at both BLA→mPFC and BLA→vHPC synapses.

Stimulation of BLA-PNs Rescues CSDS-Induced Social Avoidance

We then assessed the role of the BLA→mPFC and BLA→vHPC pathways in defeat-induced depressive-like behaviors by injecting AAV5-hSyn-hChR2-EYFP into the BLA (Figure 2A) and implanting optic fibers in the ChR2 (channelrhodopsin-2)-infected axon terminals in the mPFC (Figure 2B) or vHPC (Figure 2D). Each mouse received 5 minutes of optic stimulation immediately after each defeat. CSDS significantly decreased social interaction with a target CD-1 mouse in control animals injected with AAV5-hSyn-EYFP, whereas BLA→mPFC photostimulation reversed the CSDS-induced social avoidance (Figure 2C). BLA→vHPC photostimulation also attenuated the CSDS-induced social impairment (Figure 2E). These data indicate that the activation of BLA→mPFC or BLA→vHPC projections is proresilient in response to CSDS.

To characterize the putative postsynaptic signaling events underlying the rescuing effects from photostimulation of the BLA projections on the CSDS-elicited social avoidance, we conducted quantitative polymerase chain reaction for various glutamate receptor subunits in the mPFC and vHPC: mGluRs *Grm1, Grm2, Grm3, Grm4, Grm5, Grm6, Grm7*, and *Grm8*; subunits of NMDA receptors *Grin1, Grin2a, Grin2b, Grin2c, Grin2d*, *Grin3a, and Grn3b*; subunits of AMPA receptors *Gria1, Gria2, Gria3*, and *Gria4*; and subunits of kainic acid receptors *Grik1, Grik2, Grik3, Grik4*, and *Grik5* (Figures S6 and S7 in Supplement 1). Among them, we found that *Grm5* was the only gene in which RNA expression was significantly decreased by CSDS but reversed by BLA→mPFC (Figure 2H) and BLA→vHPC (Figure 2K) stimulation. Similar to the quantitative polymerase chain reaction data, additional Western blotting analyses showed similar expression patterns of mGluR5 proteins in the mPFC (Figure 2F, G) and vHPC (Figure 2I, J). These data suggest that mGluR5 expression in the mPFC and vHPC is modulated BLA circuit activity.

Inhibition of BLA-PNs Has Prodepressive-like Effects

To address whether inactivation of BLA→mPFC and BLA→vHPC projections promotes vulnerability to defeat stress in contrast to the proresilient effect by photoactivation of BLA projections, we injected AAV5-hSyn-eNpHR3.0-EYFP into BLA neurons (Figure 3A), and 2 weeks later, the optic fibers were implanted into the mPFC or vHPC (Figure 3B, D). The 1-day SSDS procedure did not reduce social interactions, as observed in previous studies (34). However, mice that received photostimulation of amber light in the mPFC (Figure 3C) or vHPC (Figure 3E) immediately after each defeat exhibited a sharp decrease in social interactions 24 hours after SSDS. In addition, our data showed that *Grm5* messenger RNA and mGluR5 protein expression were downregulated by SSDS with photoinactivation of BLA→mPFC (Figure 3F–H) or BLA→vHPC (Figure 3I–K) projections. These results indicate that inactivation of the BLA→mPFC or BLA→vHPC circuits by SSDS promotes depressive-like behavioral abnormalities and reductions of mGluR5.

Functional Independence of BLA Projections in Depressive-like Behaviors

Next, we investigated interaction of BLA projections in depressive-like behaviors in response to CSDS. For simultaneous photoactivation of BLA→mPFC and BLA→vHPC projections, we injected AAV5-hSyn-hChR2-EYFP into the BLA, and 2 weeks later, optic fibers were implanted in the mPFC and vHPC regions (Figure 4A, B). Each mouse received 5 minutes of ChR2 photoactivation immediately after each defeat. Each photoactivation of BLA→mPFC and or BLA→vHPC projections successfully reversed CSDS-induced social

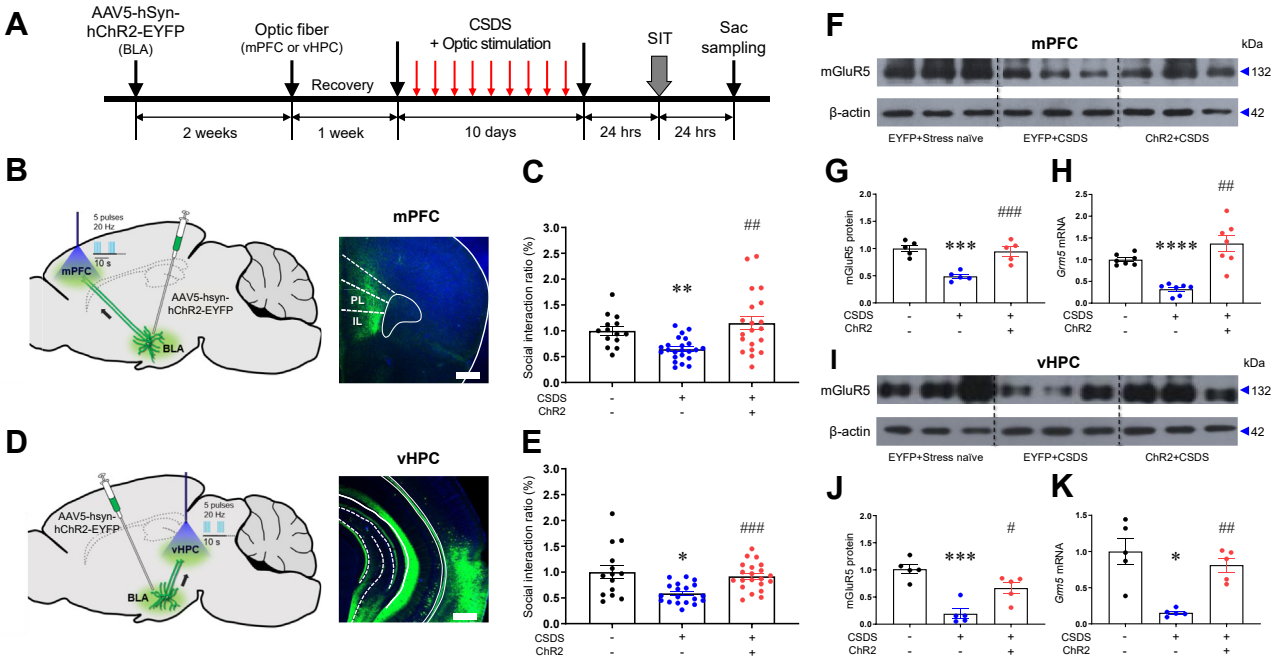

Figure 2. Activation of BLA projections in social behaviors and mGluR5 expression in response to CSDS. **(A)** Experimental procedures for ChR2 stimulation of the BLA→mPFC or BLA→vHPC pathways. **(B, D)** AAV5-hSyn-hChR2(H134R)-EYFP was injected into the BLA, and optic fibers were implanted into the mPFC or vHPC. Scale bars = 500 μm. **(C, E)** Photoactivation of the BLA→mPFC circuit significantly reversed social avoidance by CSDS (one-way ANOVA with Welch's test, $F_{2,33.47} = 8.663$, $p = .0009$, $n = 14, 24, 20$). BLA→vHPC photoactivation also prevented social avoidance by CSDS (one-way ANOVA with Welch's test, $F_{2,33.47} = 6.801$, $p = .0047$, $n = 14, 19, 21$). **(F, G)** Typical immunoblots with quantification for mGluR5 protein expression in the mPFC of EYFP+stress-naïve, EYFP+CSDS, and ChR2+CSDS mice. EYFP+CSDS mice showed reduced mGluR5 protein expression, which was blocked by BLA→mPFC activation during CSDS (ChR2+CSDS) (one-way ANOVA with Tukey's test, $F_{2,12} = 18.26$, $p = .0002$, $n = 5$). **(H)** Consistently, CSDS decreased *Grm5* mRNA expression, which was rescued by BLA→mPFC activation (one-way ANOVA with Welch's test, $F_{2,7.595} = 21.34$, $p = .0008$, $n = 5$). **(I, J)** Similarly to the mPFC, reduced levels of mGluR5 proteins in the vHPC by CSDS were alleviated by BLA→vHPC activation during CSDS (one-way ANOVA with Tukey's test, $F_{2,12} = 19.56$, $p = .0002$, $n = 5$). **(K)** *Grm5* mRNA levels also decreased after CSDS, whose effects were blocked by BLA→vHPC activation (one-way ANOVA with Welch's test, $F_{2,6.149} = 13.32$, $p = .0058$, $n = 5$). Post hoc analysis, $^{*}p < .05$, $^{**}p < .01$, $^{***}p < .001$, $^{****}p < .0001$ compared with the control+EYFP group; $^{\#}p < .05$, $^{\#\#}p < .01$, $^{\#\#\#}p < .001$ compared with the CSDS+EYFP group. Data represented as mean ± SEM. ANOVA, analysis of variance; BLA, basolateral amygdala; ChR2, channelrhodopsin-2; CSDS, chronic social defeat stress; EYFP, enhanced yellow fluorescent protein; IL, infralimbic; mGluR5, metabotropic glutamate receptor 5; mPFC, medial prefrontal cortex; mRNA, messenger RNA; PL, prelimbic; SIT, social interaction test; vHPC, ventral hippocampus.

avoidance (Figure 4C) and anhedonic behavior, as measured in the sucrose preference test (Figure 4D). However, simultaneous activation of these two BLA neural circuits did not further ameliorate CSDS-induced depressive-like behaviors compared with photoactivation of each BLA circuit, indicating no synergic effects. These results suggest that BLA→mPFC and or BLA→vHPC projections play proresilient roles in response to CSDS in an independent way despite BLA neurons co-projecting to the mPFC and vHPC, as in Figure S3F in Supplement 1.

For cross-photomanipulations of the BLA→mPFC and BLA→vHPC circuits, we injected both AAV5-hSyn-hChR2-EYFP and AAV5-hSyn-eNpHR3.0-EYFP into the BLA, and 2 weeks later, optic fibers were implanted in the mPFC and vHPC (Figure 4E). Each mouse underwent a photoinactivation of the BLA→mPFC circuits and photoactivation of the BLA→vHPC circuits at the same time, immediately after receiving defeat (Figure 4F). Photostimulation of the BLA→vHPC circuits successfully blocked CSDS-induced social avoidance (Figure 4G) and anhedonic behavior (Figure 4H), as in Figure 2E. However, photoinhibition of the BLA→mPFC circuits did not aggravate CSDS-induced social avoidance (Figure 4G) and anhedonic behavior (Figure 4H), suggesting a possibility of the ceiling effect. However, the reversal effects of BLA→vHPC PN photostimulation on CSDS-induced depressive-like behaviors were also not affected by BLA→mPFC PN photoinhibition. Likewise, the photostimulation of BLA→mPFC circuits reversed the CSDS-induced social avoidance (Figure 4J), as observed in Figure 2D. The reversal effects of the BLA→mPFC PN photostimulation on CSDS-induced depressive-like behaviors were also not affected by the BLA→vHPC PN photoinhibition. Together, these data suggest the functional independence of these two BLA projections.

Proresilient Role of mGluR5 in Behavioral Responses to CSDS

To determine whether mGluR5 has proresilient effects in response to CSDS, we first overexpressed mGluR5 by injecting LV-EF1α-mGluR5-IRES-ZsGreen1 into the mPFC and vHPC (Figure 5A, B; Figure S8A, C in Supplement 1). When mice were evaluated for their social interaction 24 hours after the last defeat, we observed that mGluR5 overexpression in

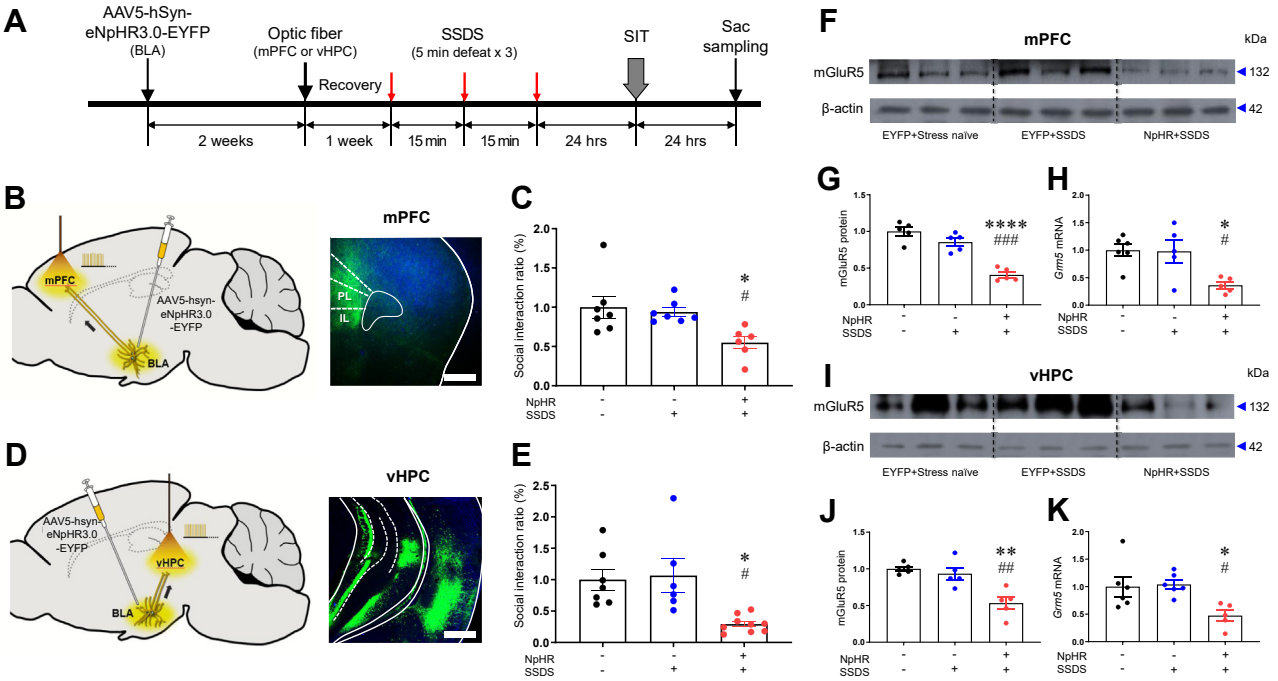

Figure 3. Inactivation of BLA projections in social behaviors and mGluR5 expression in response to CSDS. **(A)** Experimental procedures for photoinactivation of the BLA→mPFC or BLA→vHPC pathways in SSDS. **(B, D)** For photoinactivation, AAV5-hSyn-eNpHR3.0-EYFP was infused into the BLA and 594 nm of constant amber light was delivered into the mPFC **(B)** or vHPC **(D)**. Scale bars = 500 μm. **(C)** Photoinactivation of the BLA→mPFC circuit significantly reduced social interaction during the SSDS procedure (Kruskal-Wallis *H* test, $H = 10.90$, $p = .0013$, $n = 7, 7, 6$). **(E)** BLA→vHPC photoinactivation also significantly induced susceptibility to SSDS (one-way ANOVA with Welch's test, $F_{2,9.238} = 6.404$, $p = .0180$, $n = 7, 6, 9$). **(F, G)** SSDS did not alter mGluR5 protein expression in the mPFC, which was decreased by BLA→mPFC inactivation (one-way ANOVA with Tukey's test, $F_{2,12} = 35.36$, $p < .0001$, $n = 5$). **(H)** *Grm5* mRNA levels in the mPFC were also reduced by BLA→mPFC inactivation during the SSDS procedure (one-way ANOVA with Tukey's test, $F_{2,13} = 35.36$, $p = .0099$, $n = 6, 5, 5$). **(I–K)** Similar to the mPFC, vHPC mGluR5 protein and mRNA levels were not changed by SSDS but decreased by BLA→vHPC inactivation during SSDS. **(J)** Protein: one-way ANOVA with Tukey's test, $F_{2,12} = 19.56$, $p = .0002$, $n = 5$. **(K)** mRNA: $F_{2,14} = 5.471$, $p = .0175$, $n = 6, 6, 5$. Post hoc analysis, $^{*}p < .05$, $^{**}p < .01$, $^{****}p < .0001$ compared with the control+EYFP group; $^{\#}p < .05$, $^{\#\#}p < .01$, $^{\#\#\#}p < .001$ compared with the SSDS+EYFP group. Data represented as mean ± SEM. ANOVA, analysis of variance; BLA, basolateral amygdala; CSDS, chronic social defeat stress; EYFP, enhanced yellow fluorescent protein; IL, infralimbic; mGluR5, metabotropic glutamate receptor 5; mPFC, medial prefrontal cortex; mRNA, messenger RNA; NpHR, halorhodopsin; PL, prelimbic; SIT, social interaction test; SSDS, subthreshold social defeat stress; vHPC, ventral hippocampus.

the mPFC and vHPC blunted CSDS-elicited social avoidance (Figure 5C, E) and anhedonic behavior (Figure 5D, F). These data suggest that mGluR5 has proresilient effects. Next, to investigate the causal link between mGluR5 expression and stress resilience, we examined whether a knockdown of mGluR5 expression in the mPFC or vHPC has prodepressive effects. We injected AAV5-hSyn1-mGluR5-shRNA-GFP into the mPFC and vHPC (Figure 5G, H; Figure S8B, D in Supplement 1). Two weeks later, the mice were exposed to SSDS. We found that mGluR5 knockdown in the mPFC or vHPC with SSDS significantly reduced social interaction (Figure 5I, K) and sucrose preference (Figure 5J, L). In addition, we investigated whether mGluR5 directly mediates the modulatory effects of the activity of BLA projections on stress-related social avoidance behaviors by blocking mGluR5 expression in the mPFC or vHPC and by photostimulating the BLA→mPFC or BLA→vHPC circuits (Figure S8E, F in Supplement 1). Notably, mGluR5 knockdown target areas completely suppressed the reversal effects of ChR2 activation of BLA→mPFC and BLA→vHPC projections on CSDS-elicited social avoidance (Figure S8G, H in Supplement 1). Together, these results suggest a critical mediating role of mGluR5 in BLA projection activities and stress-related social behaviors.

Pharmacological Modulation of mGluR5 Downstream Signaling Affects Depressive-like Behaviors

Postsynaptic mGluR5 initiates a variety of downstream signaling pathways, mainly via the canonical G_q-dependent mechanism, generating inositol-1, 4, 5-trisphosphate and diacylglycerol, which typically activate protein kinase C (PKC). mGluR5-ERK coupling can occur not only via G_q-dependent mechanisms (G_q-PKC-ERK) but also via G_q-independent (or Homer1b/c-dependent) mechanisms (41,42). In addition, mGluR5 signaling can activate other pathways, such as the PI3K/Akt/mechanistic target of rapamycin kinase pathway through a G_q-independent mechanism (Homer1b/c-PI3K-Akt) (43,44). Because a wide range of mGluR5 downstream signaling pathways can explain social avoidance, we next evaluated the activation and protein levels of several mGluR5 signaling components in the mPFC or vHPC using Western blotting analyses. We observed reduced mGluR5

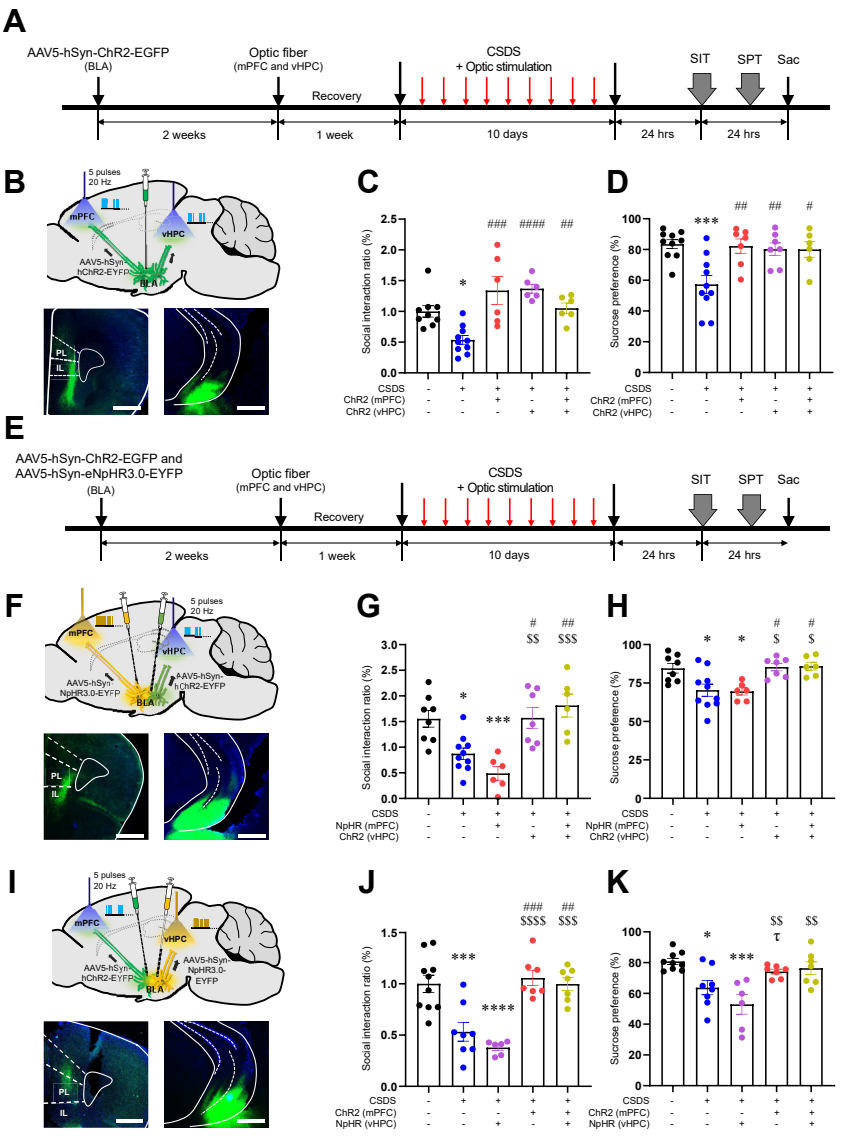

Figure 4. Null interaction of BLA projections in depressive-like behaviors in response to CSDS. **(A)** Experimental procedures for simultaneous photoactivation of BLA→mPFC and BLA→vHPC pathways in CSDS. **(B)** AAV5-hSyn-hChR2(H134R)-EYFP was injected into the BLA, and optic fibers were implanted into both the mPFC and vHPC. Scale bars = 800 μm. **(C, D)** Photoactivation of the BLA→mPFC and/or BLA→vHPC circuits significantly reversed CSDS-induced social avoidance **(C)** (Kruskal-Wallis H test, $H = 28$, $p = .0003$, $n = 9, 10, 6, 6, 6$) and anhedonic behavior, which was measured by SPT **(D)** (one-way ANOVA with Tukey's test, $F_{4,35} = 6.527$, $p = .0005$, $n = 10, 10, 7, 7, 6$). Of note, the photoactivation effects of either of the BLA pathways were not different from the simultaneous photoactivation effects of both BLA pathways, suggesting null synergic interaction of those BLA circuits on depressive-like behaviors. **(E)** Experimental procedures for cross-photomanipulation of BLA→mPFC and BLA→vHPC pathways in CSDS. **(F, I)** After AAV5-hSyn-hChR2(H134R)-EYFP and AAV5-hSyn-eNpHR3.0-EYFP were injected into the BLA, we implanted optic fibers for photoinhibition into the mPFC and those for photoactivation into the vHPC and vice versa. Scale bars = 800 μm. **(G, H)** CSDS-induced social avoidance and anhedonic behavior were not aggravated by NpHR photoinactivation over the BLA→mPFC circuit but reversed by ChR2 activation over the BLA→vHPC circuit. **(G)** Social interaction: one-way ANOVA with Tukey's test, $F_{4,32} = 10.39$, $p < .0001$, $n = 8, 10, 6, 7, 6$. **(H)** Sucrose preference: $F_{4,32} = 6.609$, $p = .0005$, $n = 8, 10, 6, 7, 6$. **(J, K)** Similarly, CSDS-induced depressive-like behaviors were not influenced by NpHR photoinactivation over the BLA→vHPC circuit but reversed by ChR2 activation over the BLA→mPFC circuit. **(J)** Social interaction: $F_{4,33} = 14.87$, $p < .0001$, $n = 10, 8, 6, 7, 7$. **(K)** Sucrose preference: one-way ANOVA with Welch's test, $F_{4,17.68} = 7.360$, $p = .0011$, $^{£}p = .0605$. $n = 9, 8, 6, 7, 7$. The reversal effects of ChR2 activation over one of either of the BLA pathways on depressive-like behaviors were not diminished by NpHR photoinactivation of the other BLA pathway, which suggests functional independence of these two BLA projections. Post hoc analysis, $^{*}p < .05$, $^{**}p < .01$, $^{***}p < .001$, $^{****}p < .0001$ compared with the control+EYFP group; $^{τ}p < .1$, $^{\#}p < .05$, $^{\#\#}p < .01$, $^{\#\#\#}p < .001$, $^{\#\#\#\#}p < .0001$ compared with the CSDS+EYFP group; $^{\$}p < .05$, $^{\$\$}p < .01$, $^{\$\$\$}p < .001$, $^{\$\$\$\$}p < .0001$ compared with the CSDS+NpHR (either mPFC or vHPC) group. Data represented as mean ± SEM. ANOVA, analysis of variance; BLA, basolateral amygdala; ChR2, channelrhodopsin-2; CSDS, chronic social defeat stress; EYFP, enhanced yellow fluorescent protein; IL, infralimbic; mPFC, medial prefrontal cortex; NpHR, halorhodopsin; PL, prelimbic; SIT, social interaction test; SPT, sucrose preference test; SSDS, subthreshold social defeat stress; vHPC, ventral hippocampus.

protein expression in both the mPFC and vHPC of susceptible, but not in resilient, mice (Figure 6A–D). Similarly, CSDS downregulated Homer1b/c expression and phosphorylation of Akt in the mPFC of susceptible mice, but not in resilient mice (Figure 6A–D). No changes were observed in pPKC and pERK levels in the mPFC. By contrast, pPKC and pERK levels in the vHPC were decreased only in susceptible animals (Figure 6A–D). No changes were observed in Homer1b/c or pAKT in the vHPC. These findings suggest that differential mGluR5 downstream signaling in the mPFC and vHPC may mediate proresilient effects in response to CSDS. mGluR5 mediates the effects of CSDS in a Homer1b/c-Akt–dependent way in the mPFC, whereas it mediates these effects in a G_q-PKC-ERK–dependent manner in the vHPC. Next, we investigated whether each mGluR5 downstream signaling influences stress-related social behaviors. Approximately 2 weeks after the implantation of the cannula bilaterally in the mPFC and vHPC, we infused a selective PI3K-Akt inhibitor, LY294002, or a highly selective inhibitor of MAPK/ERK kinase, U0126, into the mPFC or vHPC. Social interaction was measured 24 hours after SSDS (Figure 6E, F). We found that the infusion of LY294002, but not of U0126, into the mPFC reduced social interaction (Figure 6G) and sucrose preference

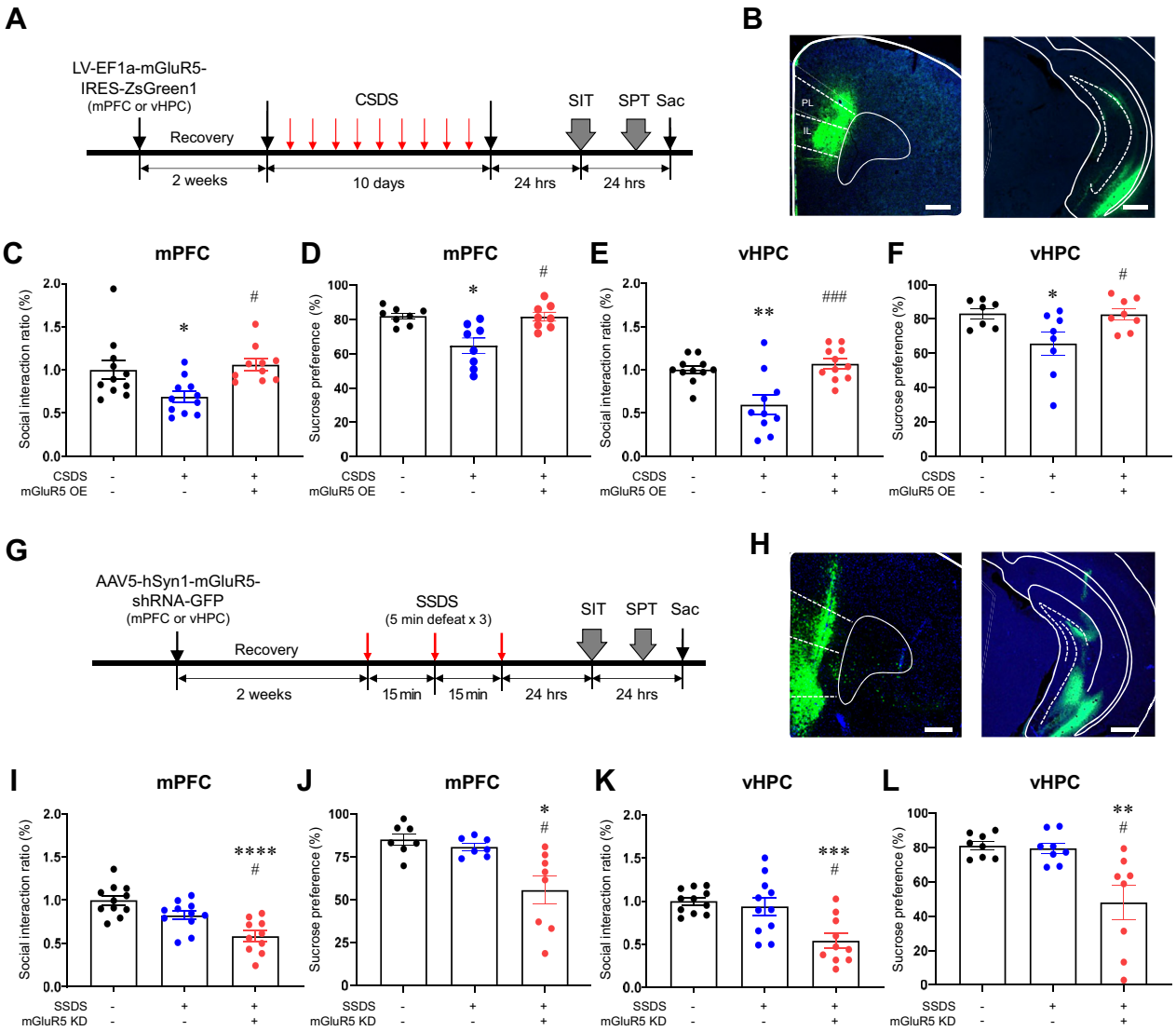

Figure 5. Role of mGluR5 in BLA projection neurons on stress resilience. **(A)** Experimental procedures for mGluR5 OE with CSDS. **(B)** Confocal images showing injection sites of LV-EF1a-mGluR5-IRES-ZsGreen1 into the mPFC and vHPC. Scale bars = 500 μm. **(C, D)** mGluR5 OE in the mPFC blocked CSDS-induced social avoidance **(C)** (Kruskal-Wallis H test, $H = 11.65$, $p = .0030$, $n = 11, 11, 10$) and anhedonic behavior **(D)** (one-way ANOVA with Tukey's test, $F_{2,21} = 9.893$, $p = .0009$, $n = 8$). **(E, F)** Similarly, mGluR5 OE in the vHPC also blocked CSDS-induced depressive-like behaviors. **(E)** Social avoidance: one-way ANOVA with Welch's test, $F_{2,17.07} = 11.00$, $p = .0009$, $n = 11, 10, 11$. **(F)** Anhedonic behavior: one-way ANOVA with Tukey's test, $F_{2,20} = 4.438$, $p = .0254$, $n = 7, 8, 8$. **(G)** Experimental procedures for mGluR5 knockdown in SSDS. **(H)** Confocal images showing injection sites of AAV5-mGluR5-shRNA into the mPFC and vHPC. Scale bars = 500 μm. **(I–L)** mGluR5 knockdown by infusion of AAV5-hSyn1-mGluR5-shRNA-GFP into the mPFC or vHPC significantly reduced the social interaction. **(I)** mPFC: one-way ANOVA with Tukey's test, $F_{2,29} = 13.97$, $p < .001$, $n = 11, 11, 10$. **(K)** vHPC: one-way ANOVA with Welch's test, $F_{2,22.27} = 9.484$, $p = .0010$, $n = 11, 11, 10$) and sucrose preference following SSDS. **(J)** mPFC: $F_{2,10.23} = 9.424$, $p = .0048$, $n = 7, 7, 8$. **(L)** vHPC: $F_{2,9.286} = 8.871$, $p = .0070$, $n = 8$. Post hoc analysis, $^{*}p < .05$, $^{**}p < .01$, $^{***}p < .001$, $^{****}p < .0001$ compared with the control+ZsGreen1/GFP group; $^{\#}p < .05$, $^{\#\#}p < .01$ compared with the CSDS/SSDS+ZsGreen1/GFP group. Data represented as mean ± SEM. ANOVA, analysis of variance; BLA, basolateral amygdala; CSDS, chronic social defeat stress; GFP, green fluorescent protein; IL, infralimbic; mGluR5, metabotropic glutamate receptor 5; mPFC, medial prefrontal cortex; OE, overexpression; PL, prelimbic; SIT, social interaction test; SPT, sucrose preference test; SSDS, subthreshold social defeat stress; vHPC, ventral hippocampus.

(Figure 6H), while the infusion of U0126, but not LY294002, into the vHPC decreased social interaction (Figure 6I) and sucrose preference (Figure 6J). These data strongly suggest that the proresilient effects of mGluR5 signaling in the mPFC and vHPC are mediated through differential downstream signaling pathways: mGluR5-Homer1b/c-pAKT signaling pathways in the mPFC versus mGluR5-G_q-pERK signaling pathways in the vHPC (Figure S9 in Supplement 1).

DISCUSSION

This study provides evidence that mGluR5 in the mPFC and vHPC that is regulated by BLA outputs can be a molecular

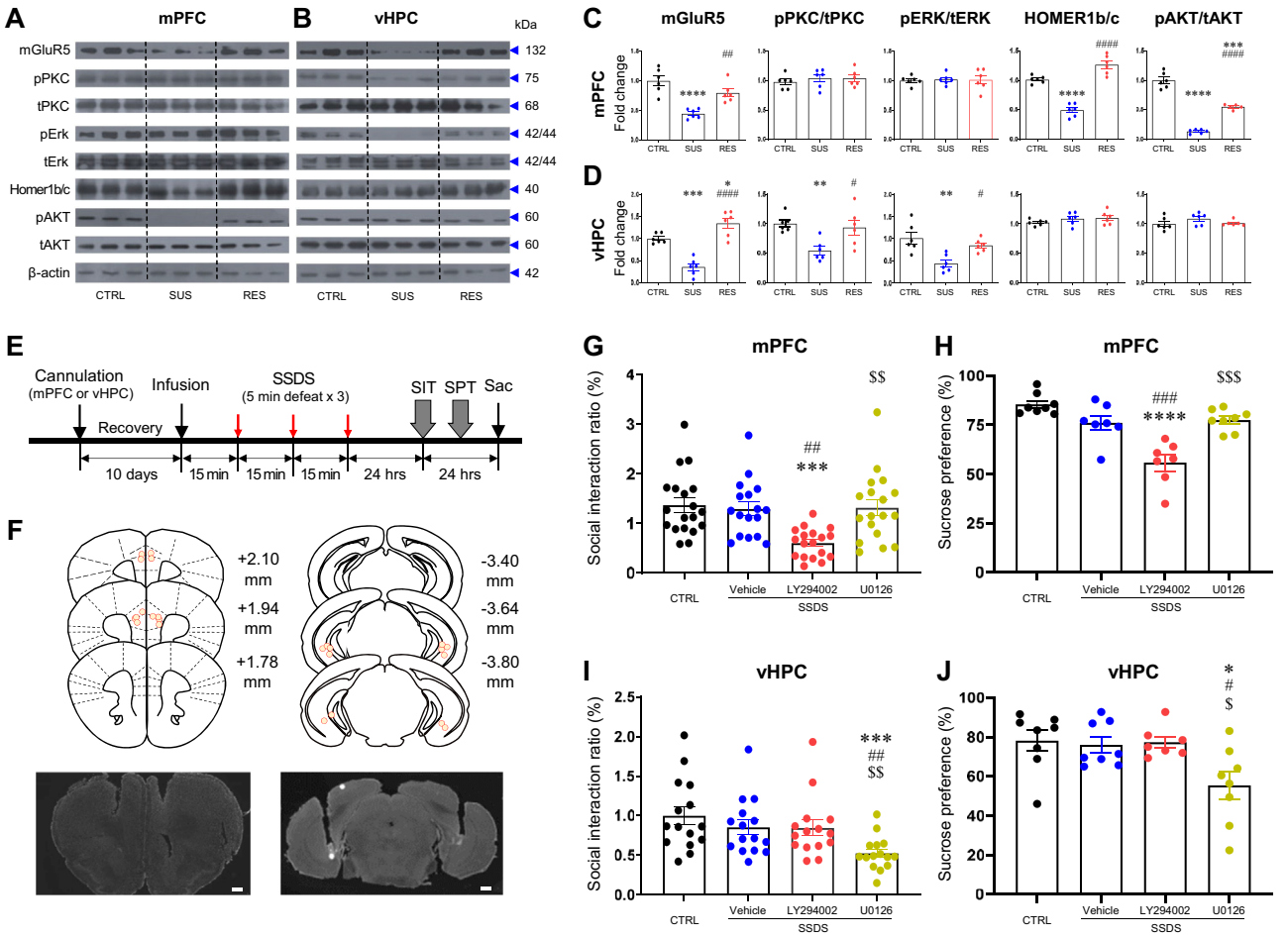

Figure 6. Distinct signaling pathways downstream to mGluR5 mediating stress resilience. **(A–D)** Representative Western blotting and quantification of mGluR5, pPKC, tPKC, pERK, tERK, Homer1b/c, pAkt, and tAkt in the mPFC **(A, C)** and vHPC **(B, D)** of CTRL, SUS, and RES mice. **(C)** mPFC protein levels of mGluR5 were decreased in SUS but not in RES mice (one-way ANOVA with Tukey's test, $F_{2,15} = 18.32$, $p < .0001$, $n = 6$). Protein levels of Homer1b/c ($F_{2,15} = 66.77$, $p < .0001$, $n = 6$) and pAKT/tAKT (one-way ANOVA with Welch's test, $F_{2,6.764} = 163.1$, $p < .0001$, $n = 6$) also decreased in the mPFC of SUS mice only, whereas pPKC/tPKC and pERK/tERK was not changed (pPKC/tPKC: $F_{2,15} = 0.4107$, $p = .6704$, $n = 6$; pERK/tERK: $F_{2,15} = 0.0362$, $p = .9645$, $n = 6$). **(D)** In the vHPC, protein levels of mGluR5 were also decreased in SUS but not in RES mice (one-way ANOVA with Tukey's test, $F_{2,15} = 33.75$, $p < .0001$, $n = 6$). In contrast to the mPFC, only SUS animals showed reduced protein levels of pPKC/tPKC ($F_{2,15} = 7.204$, $p = .0064$, $n = 6$) and pERK/tERK ($F_{2,15} = 9.444$, $p = .0022$, $n = 6$) but no changes in protein levels of Homer1b/c ($F_{2,15} = 1.178$, $p = .3349$, $n = 6$) and pAKT/tAKT (Kruskal-Wallis H test, $H = 3.193$, $p = .2128$, $n = 6$). Post hoc analysis, $^{*}p < .05$, $^{**}p < .01$, $^{***}p < .001$, $^{****}p < .0001$ compared with the CTRL group; $^{\#}p < .05$, $^{\#\#}p < .01$, $^{\#\#\#\#}p < .0001$ compared with the SUS group. **(E)** Experimental procedures for pharmacological inhibition of mGluR5 signals during SSDS. **(F)** Representative images of cannula implant sites in the mPFC and vHPC. Scale bars = 1 mm. **(G, H)** Infusion of LY294002 into the mPFC significantly reduced social interaction **(G)** (one-way ANOVA with Welch's test, $F_{3,56.48} = 7.360$, $p = .0003$, $n = 19, 17, 18, 18$) and sucrose preference **(H)** (one-way ANOVA with Tukey's test, $F_{3,26} = 17.62$, $p < .0001$, $n = 8, 7, 7, 8$) after SSDS, but U012 did not. **(I, J)** However, infusion of U012 into the vHPC induced social avoidance **(I)** (Kruskal-Wallis H test, $H = 15.19$, $p = .017$, $n = 15$) and anhedonic behavior **(J)** (one-way ANOVA with Tukey's test, $F_{3,27} = 4.572$, $p = .0103$, $n = 8, 8, 7, 8$) after SSDS, but LY294002 did not. Post hoc analysis, $^{*}p < .05$, $^{***}p < .001$, $^{****}p < .0001$ compared with the CTRL+vehicle group; $^{\#}p < .05$, $^{\#\#}p < .01$, $^{\#\#\#}p < .001$ compared with the SSDS+vehicle group; $^{\$}p < .05$, $^{\$\$}p < .01$, $^{\$\$\$}p < .001$ compared with the SSDS+LY294002 group. Data represented as mean ± SEM. ANOVA, analysis of variance; CTRL, control; mGluR5, metabotropic glutamate receptor 5; mPFC, medial prefrontal cortex; pAkt, phosphorylated protein kinase B; pERK, phosphorylated extracellular signal–regulated kinase; pPKC, phosphorylated protein kinase C; RES, resilient; SIT, social interaction test; SPT, sucrose preference test; SSDS, subthreshold social defeat stress; SUS, susceptible; tAkt, total protein kinase B; tERK, total extracellular signal–regulated kinase; tPKC, total protein kinase C; vHPC, ventral hippocampus.

switch of susceptibility to resilience in response to CSDS. Our findings show that CSDS, an ethologically validated model of aspects of depression in mice (31), decreases the activity of BLA innervations to the mPFC and vHPC, which is also observed in patients with depression (45,46). Optogenetic manipulation of BLA projection activity to the mPFC or vHPC reversed CSDS-induced mGluR5 reduction and depressive-like behaviors as measured by social interaction and sucrose preference tests. Consistently, viral-mediated mGluR5 induction alleviated CSDS-induced social avoidance and anhedonia. Furthermore, we observed that selective blockade of the distinctive mGluR5 downstream signaling pathways attenuated CSDS-elicited depressive-like behaviors in a region-specific manner. Overall, our findings indicate that mGluR5

and its selective downstream signaling in the mPFC and vHPC, which are innervated by BLA projections, are proresilient in response to CSDS.

Although the BLA and its connections with other major limbic components such as the PFC and HPC have long been implicated in the regulation of emotion and etiology of stress-related psychiatric diseases (47), there are only limited investigations on the roles of BLA projections in stress-related depressive-like behaviors. Consistent with our data, a recent study demonstrated that depressive behaviors induced by chronic immobilization stress were mediated by hypoactive glutamatergic neurons in the mPFC (48). Other studies have shown that stimulating BLA→vHPC circuits rescues depressive-like behaviors following repeated foot shock or chronic unpredictable mild stress, which weakens the BLA-vHPC connectivity (13,14). These findings highlight the proresilient role of BLA→mPFC and BLA→vHPC projections in animal models of depression using chronic stress. Furthermore, our data in this study suggest that these two BLA circuits that play the same proresilient role act in a functionally independent way: the proresilient effect of optogenetic stimulation over one of either of the BLA projections was not influenced by optogenetic manipulations (i.e., stimulation and inhibition) over the other BLA projection. Such functional independence for the same behavioral output might be associated with topographically different distributions or connectivity characteristics of BLA PNs, as observed in our study and others (49–52). However, it is noteworthy that the mPFC and vHPC give glutamatergic projections to the nucleus accumbens, which also receives projections from the BLA and other brain structures, forming a complex neural network for depressive-like behaviors (53–55). Thus, further investigation of putative interactions in this complex is required for a comprehensive understanding of the BLA circuitry functions in response to CSDS (56,57).

In this study, CSDS-induced hypoactivity of the BLA→mPFC and BLA→vHPC circuits and its concomitant depressive behaviors may occur through reductions in glutamate release at BLA→mPFC or BLA→vHPC synapses, assessed by PPRs of the excitatory postsynaptic current following pathway-specific stimulation. Our findings are in line with earlier preclinical evidence showing that glutamine supplementation reverses reduced levels of glutamate/glutamine cycling or glutamatergic activity in the PFC of chronically stressed mice, thereby attenuating stress-induced depressive-like behaviors (48,58,59). Clinical studies have also shown reduced glutamate metabolite levels in the PFC and HPC of patients with depression (60,61). This suggests a critical role of glutamatergic transmission at BLA terminals in depressive-like behaviors.

It is worth noting that mGluR5 is the only glutamate receptor subtype whose expression is decreased by CSDS and reversed by the stimulation of BLA projections. The expression of glutamate receptors such as *Grin2a, Gria1, Gria2, Gria3*, and/or *Gria4* was also reduced in the mPFC and vHPC of stressed mice, but BLA activation had no reversal effects. These data suggest that mGluR5 in the BLA PN targets, such as mPFC and vHPC, is the only receptor that can regulate the detrimental effects of CSDS on depressive-like behaviors in a BLA PN activity–dependent manner. Indeed, such mGluR5 alterations were compatible with social avoidance and anhedonic behaviors that were induced by CSDS but reversed by the BLA circuit stimulation. Consistently, we found a regulatory effect of viral-mediated mGluR5 induction in the mPFC and vHPC on CSDS-induced depressive-like behaviors.

We further observed that mGluR5 knockdown in both the mPFC and vHPC completely blocked the reversal effects from photoactivation of BLA projections on CSDS-induced depressive-like behavior. This supports a scheme wherein mGluR5 is a key mediator of the proresilient effects of the BLA circuit activation on depressive-like behaviors in response to CSDS. It is of particular interest that the resilient effects of mGluR5 are distinctively mediated by G_q-independent Homer1b/c-Akt signaling in the mPFC and by G_q-dependent PKC-ERK signaling in the vHPC. These data are not consistent with previous studies showing enhanced mGluR5 and Homer1b/c expressions in the dorsal hippocampus of CSDS- SUS mice (62,63). This could be due to differences in connectivity-based functions in the dorsal HPC, which primarily performs cognitive functions, and in the vHPC, which performs functions related to stress and emotion (64).

In conclusion, our study demonstrates a proresilient role of mGluR5 signaling in the mPFC and vHPC innervated by the BLA in social behaviors affected by CSDS. The sustained inactivation of BLA PNs, in the context of stress, suppresses postsynaptic mGluR5, which may produce pathological effects, as observed in patients with depression (19). However, proresilient mGluR5 signaling in BLA outputs is likely in contrast to the antidepressant effects of mGluR5 antagonists or mGluR5 deletion (20,65). These inconsistencies may be due to the diverse roles of mGluR5 in specific neuronal populations, regions, and circuits, which are differentially modulated by various stresses (29,66,67), and require further study. Sex-specific physiological characteristics of mGluR5 in depression also need to be further investigated. It may be difficult to explore this system in female subjects with depression because of the more noticeable circadian variation of mGluR5 availability in female subjects and circadian misalignment in subjects with depression (18,68,69). However, such an investigation would be a crucial step toward the development or optimization of precision interventions to treat depression, especially for women, who show a higher lifetime prevalence of depression than men (70,71).

ACKNOWLEDGMENTS AND DISCLOSURES

This work was supported by the National Research Foundation of Korea (Grant Nos. 2016M3C7A1914451 and 2020M3A9E4104384 [to K-AC] and Grant Nos. 2017M3C7A1048089 and 2018M3C7A1024150 [to JWK]) and the Korea Brain Research Institute (KBRI) Basic Research Program (Grant No. 21-BR-02-06 [to JWK]).

JK, SK, T-YC, K-AC, and JWK jointly conceived and designed the study. JK and SK performed the ChR2, NpHR, Jaws, and Lenti shRNA virus surgery; histological analysis; and social interaction tests and analyzed the data. JK and SK performed chronic social defeat stress and optogenetics. JK performed subthreshold social defeat stress, forced swim test, sucrose preference test, real-time reverse transcriptase polymerase chain reaction (RT-PCR), and drug cannula infusion. T-YC performed the electrophysiological experiments. JK and SK collected tissue samples and performed RT-PCR and Western blotting, respectively. JK, SK, K-AC, and JWK wrote the manuscript. All authors discussed and commented on the manuscript and approved the final submission.

We thank Chul Hoon Kim (Yonsei University College of Medicine) for providing the lentiviral vectors and Tae-Eun Kim (KBRI and Daegu Gyeongbuk Institute of Science and Technology), Yoo Jin Lee (KBRI), and Hyang-Sook Hoe (KBRI) for their technical support.

The authors report no biomedical financial interests or potential conflicts of interest.

ARTICLE INFORMATION

From the Emotion, Cognition and Behavior Research Group (JK, T-YC, JWK), Korea Brain Research Institute; Department of Brain and Cognitive Sciences (JK, JWK), Daegu Gyeongbuk Institute of Science and Technology, Daegu; Department of Pharmacology (SK, K-AC), College of Medicine; Neuroscience Research Institute (SK, K-AC); Department of Health Sciences and Technology (SK, K-AC), GAIHST, Gachon University, Incheon, Republic of Korea; and the Department of Molecular Pharmacology and Experimental Therapeutics (SK), Mayo Clinic, Rochester, Minnesota.

JK and SK contributed equally to this work.

K-AC and JWK contributed equally to this work.

Address correspondence to Keun-A Chang, Ph.D., at keuna705@gachon.ac.kr, or Ja Wook Koo, Ph.D., at jawook.koo@kbri.re.kr.

Received Mar 29, 2021; revised Jan 10, 2022; accepted Jan 13, 2022.

Supplementary material cited in this article is available online at https://doi.org/10.1016/j.biopsych.2022.01.006.

REFERENCES

1. GBD 2017 Disease and Injury Incidence and Prevalence Collaborators (2018): Global, regional, and national incidence, prevalence, and years lived with disability for 354 diseases and injuries for 195 countries and territories, 1990–2017: A systematic analysis for the Global Burden of Disease Study 2017 [published correction appears in Lancet 2019; 393:e44]. Lancet 392:1789–1858.
2. Kessler RC (1997): The effects of stressful life events on depression. Annu Rev Psychol 48:191–214.
3. Kendler KS, Karkowski LM, Prescott CA (1999): Causal relationship between stressful life events and the onset of major depression. Am J Psychiatry 156:837–841.
4. Feder A, Nestler EJ, Charney DS (2009): Psychobiology and molecular genetics of resilience. Nat Rev Neurosci 10:446–457.
5. Han MH, Nestler EJ (2017): Neural substrates of depression and resilience. Neurotherapeutics 14:677–686.
6. Reus GZ, de Moura AB, Silva RH, Resende WR, Quevedo J (2018): Resilience dysregulation in major depressive disorder: Focus on glutamatergic imbalance and microglial activation. Curr Neuropharmacol 16:297–307.
7. McEwen BS, Gray J, Nasca C (2015): Recognizing resilience: Learning from the effects of stress on the brain. Neurobiol Stress 1:1–11.
8. Zhang WH, Zhang JY, Holmes A, Pan BX (2021): Amygdala circuit substrates for stress adaptation and adversity. Biol Psychiatry 89:847–856.
9. Tye KM (2018): Neural circuit motifs in valence processing. Neuron 100:436–452.
10. O'Neill PK, Gore F, Salzman CD (2018): Basolateral amygdala circuitry in positive and negative valence. Curr Opin Neurobiol 49:175–183.
11. Felix-Ortiz AC, Tye KM (2014): Amygdala inputs to the ventral hippocampus bidirectionally modulate social behavior. J Neurosci 34:586–595.
12. Liu WZ, Zhang WH, Zheng ZH, Zou JX, Liu XX, Huang SH, *et al.* (2020): Identification of a prefrontal cortex-to-amygdala pathway for chronic stress-induced anxiety. Nat Commun 11:2221.
13. Ma H, Li C, Wang J, Zhang X, Li M, Zhang R, *et al.* (2021): Amygdala-hippocampal innervation modulates stress-induced depressive-like behaviors through AMPA receptors. Proc Natl Acad Sci U S A 118: e2019409118.
14. Yang Y, Wang ZH, Jin S, Gao D, Liu N, Chen SP, *et al.* (2016): Opposite monosynaptic scaling of BLP–vCA1 inputs governs hopefulness- and helplessness-modulated spatial learning and memory. Nat Commun 7:11935.
15. Burgos-Robles A, Kimchi EY, Izadmehr EM, Porzenheim MJ, Ramos-Guasp WA, Nieh EH, *et al.* (2017): Amygdala inputs to prefrontal cortex guide behavior amid conflicting cues of reward and punishment. Nat Neurosci 20:824–835.
16. Duman RS, Sanacora G, Krystal JH (2019): Altered connectivity in depression: GABA and glutamate neurotransmitter deficits and reversal by novel treatments. Neuron 102:75–90.
17. Lener MS, Niciu MJ, Ballard ED, Park M, Park LT, Nugent AC, Zarate CA Jr (2017): Glutamate and gamma-aminobutyric acid systems in the pathophysiology of major depression and antidepressant response to ketamine. Biol Psychiatry 81:886–897.
18. Esterlis I, Holmes SE, Sharma P, Krystal JH, DeLorenzo C (2018): Metabotropic glutamatergic receptor 5 and stress disorders: Knowledge gained from receptor imaging studies. Biol Psychiatry 84:95–105.
19. Terbeck S, Akkus F, Chesterman LP, Hasler G (2015): The role of metabotropic glutamate receptor 5 in the pathogenesis of mood disorders and addiction: Combining preclinical evidence with human positron emission tomography (PET) studies. Front Neurosci 9:86.
20. Krystal JH, Mathew SJ, D'Souza DC, Garakani A, Gunduz-Bruce H, Charney DS (2010): Potential psychiatric applications of metabotropic glutamate receptor agonists and antagonists. CNS Drugs 24:669–693.
21. Abdallah CG, Hannestad J, Mason GF, Holmes SE, DellaGioia N, Sanacora G, *et al.* (2017): Metabotropic glutamate receptor 5 and glutamate involvement in major depressive disorder: A multimodal imaging study. Biol Psychiatry Cogn Neurosci Neuroimaging 2:449–456.
22. Kim JH, Joo YH, Son YD, Kim JH, Kim YK, Kim HK, *et al.* (2019): In vivo metabotropic glutamate receptor 5 availability-associated functional connectivity alterations in drug-naïve young adults with major depression. Eur Neuropsychopharmacol 29:278–290.
23. Deschwanden A, Karolewicz B, Feyissa AM, Treyer V, Ametamey SM, Johayem A, *et al.* (2011): Reduced metabotropic glutamate receptor 5 density in major depression determined by [(11)C]ABP688 PET and postmortem study. Am J Psychiatry 168:727–734.
24. Howard DM, Adams MJ, Shirali M, Clarke TK, Marioni RE, Davies G, *et al.* (2018): Genome-wide association study of depression phenotypes in UK Biobank identifies variants in excitatory synaptic pathways [published correction appears in Nat Commun 2021; 12:2012]. Nat Commun 9:1470.
25. Iyo AH, Feyissa AM, Chandran A, Austin MC, Regunathan S, Karolewicz B (2010): Chronic corticosterone administration down-regulates metabotropic glutamate receptor 5 protein expression in the rat hippocampus. Neuroscience 169:1567–1574.
26. Wierońska JM, Brański P, Szewczyk B, Pałucha A, Papp M, Gruca P, *et al.* (2001): Changes in the expression of metabotropic glutamate receptor 5 (mGluR5) in the rat hippocampus in an animal model of depression. Pol J Pharmacol 53:659–662.
27. Kovačević T, Skelin I, Minuzzi L, Rosa-Neto P, Diksic M (2012): Reduced metabotropic glutamate receptor 5 in the Flinders Sensitive Line of rats, an animal model of depression: An autoradiographic study. Brain Res Bull 87:406–412.
28. Shin S, Kwon O, Kang JI, Kwon S, Oh S, Choi J, *et al.* (2015): mGluR5 in the nucleus accumbens is critical for promoting resilience to chronic stress. Nat Neurosci 18:1017–1024.
29. Lee KW, Westin L, Kim J, Chang JC, Oh YS, Amreen B, *et al.* (2015): Alteration by p11 of mGluR5 localization regulates depression-like behaviors. Mol Psychiatry 20:1546–1556.
30. Krishnan V, Han MH, Graham DL, Berton O, Renthal W, Russo SJ, *et al.* (2007): Molecular adaptations underlying susceptibility and resistance to social defeat in brain reward regions. Cell 131:391–404.
31. Krishnan V, Nestler EJ (2011): Animal models of depression: Molecular perspectives. Curr Top Behav Neurosci 7:121–147.
32. Koo JW, Labonté B, Engmann O, Calipari ES, Juarez B, Lorsch Z, *et al.* (2016): Essential role of mesolimbic brain-derived neurotrophic factor in chronic social stress-induced depressive behaviors. Biol Psychiatry 80:469–478.

33. Walsh JJ, Friedman AK, Sun H, Heller EA, Ku SM, Juarez B, *et al.* (2014): Stress and CRF gate neural activation of BDNF in the mesolimbic reward pathway. Nat Neurosci 17:27–29.
34. Chaudhury D, Walsh JJ, Friedman AK, Juarez B, Ku SM, Koo JW, *et al.* (2013): Rapid regulation of depression-related behaviours by control of midbrain dopamine neurons. Nature 493:532–536.
35. Barth AL, Gerkin RC, Dean KL (2004): Alteration of neuronal firing properties after in vivo experience in a FosGFP transgenic mouse. J Neurosci 24:6466–6475.
36. Morgan JI, Cohen DR, Hempstead JL, Curran T (1987): Mapping patterns of c-fos expression in the central nervous system after seizure. Science 237:192–197.
37. Goldstein L (1992): The Amygdala: Neurobiological Aspects of Emotion, Memory, and Mental Dysfunction. Yale J Biol Med 65:540–542.
38. Liu J, Hu T, Zhang MQ, Xu CY, Yuan MY, Li RX (2021): Differential efferent projections of GABAergic neurons in the basolateral and central nucleus of amygdala in mice. Neurosci Lett 745:135621.
39. Manabe T, Wyllie DJ, Perkel DJ, Nicoll RA (1993): Modulation of synaptic transmission and long-term potentiation: Effects on paired pulse facilitation and EPSC variance in the CA1 region of the hippocampus. J Neurophysiol 70:1451–1459.
40. Dobrunz LE, Stevens CF (1997): Heterogeneity of release probability, facilitation, and depletion at central synapses. Neuron 18:995–1008.
41. Mao L, Yang L, Tang Q, Samdani S, Zhang G, Wang JQ (2005): The scaffold protein Homer1b/c links metabotropic glutamate receptor 5 to extracellular signal-regulated protein kinase cascades in neurons. J Neurosci 25:2741–2752.
42. Stoppel LJ, Auerbach BD, Senter RK, Preza AR, Lefkowitz RJ, Bear MF (2017): β-Arrestin2 couples metabotropic glutamate receptor 5 to neuronal protein synthesis and is a potential target to treat fragile X. Cell Rep 18:2807–2814.
43. Olmo IG, Ferreira-Vieira TH, Ribeiro FM (2016): Dissecting the signaling pathways involved in the crosstalk between metabotropic glutamate 5 and cannabinoid type 1 receptors. Mol Pharmacol 90:609–619.
44. Holz A, Mülsch F, Schwarz MK, Hollmann M, Döbrössy MD, Coenen VA, *et al.* (2019): Enhanced mGlu5 signaling in excitatory neurons promotes rapid antidepressant effects via AMPA receptor activation. Neuron 104:338–352.e7.
45. Tang Y, Kong L, Wu F, Womer F, Jiang W, Cao Y, *et al.* (2013): Decreased functional connectivity between the amygdala and the left ventral prefrontal cortex in treatment-naive patients with major depressive disorder: A resting-state functional magnetic resonance imaging study. Psychol Med 43:1921–1927.
46. Cullen KR, Westlund MK, Klimes-Dougan B, Mueller BA, Houri A, Eberly LE, Lim KO (2014): Abnormal amygdala resting-state functional connectivity in adolescent depression [published correction appears in JAMA Psychiatry 2018; 75:104]. JAMA Psychiatry 71:1138–1147.
47. Ulrich-Lai YM, Herman JP (2009): Neural regulation of endocrine and autonomic stress responses. Nat Rev Neurosci 10:397–409.
48. Son H, Baek JH, Go BS, Jung DH, Sontakke SB, Chung HJ, *et al.* (2018): Glutamine has antidepressive effects through increments of glutamate and glutamine levels and glutamatergic activity in the medial prefrontal cortex. Neuropharmacology 143:143–152.
49. McGarry LM, Carter AG (2017): Prefrontal cortex drives distinct projection neurons in the basolateral amygdala. Cell Rep 21:1426–1433.
50. Hintiryan H, Bowman I, Johnson DL, Korobkova L, Zhu M, Khanjani N, *et al.* (2021): Connectivity characterization of the mouse basolateral amygdalar complex. Nat Commun 12:2859.
51. Beyeler A, Chang CJ, Silvestre M, Lévêque C, Namburi P, Wildes CP, Tye KM (2018): Organization of valence-encoding and projection-defined neurons in the basolateral amygdala. Cell Rep 22:905–918.
52. Pi G, Gao D, Wu D, Wang Y, Lei H, Zeng W, *et al.* (2020): Posterior basolateral amygdala to ventral hippocampal CA1 drives approach behaviour to exert an anxiolytic effect. Nat Commun 11:183.
53. Bagot RC, Parise EM, Peña CJ, Zhang HX, Maze I, Chaudhury D, *et al.* (2015): Ventral hippocampal afferents to the nucleus accumbens regulate susceptibility to depression [published correction appears in Nat Commun 2015; 6:7626]. Nat Commun 6:7062.
54. Nestler EJ (2015): Role of the brain's reward circuitry in depression: Transcriptional mechanisms. In: De Biasi M, editor. Nicotine Use in Mental Illness and Neurological Disorders, vol. 124. Waltham, MA: Academic Press, 151–170.
55. Dieterich A, Floeder J, Stech K, Lee J, Srivastava P, Barker DJ, Samuels BA (2021): Activation of basolateral amygdala to nucleus accumbens projection neurons attenuates chronic corticosterone-induced behavioral deficits in male mice. Front Behav Neurosci 15:643272.
56. Muir J, Lopez J, Bagot RC (2019): Wiring the depressed brain: Optogenetic and chemogenetic circuit interrogation in animal models of depression. Neuropsychopharmacology 44:1013–1026.
57. Knowland D, Lim BK (2018): Circuit-based frameworks of depressive behaviors: The role of reward circuitry and beyond. Pharmacol Biochem Behav 174:42–52.
58. Banasr M, Chowdhury GMI, Terwilliger R, Newton SS, Duman RS, Behar KL, Sanacora G (2010): Glial pathology in an animal model of depression: Reversal of stress-induced cellular, metabolic and behavioral deficits by the glutamate-modulating drug riluzole. Mol Psychiatry 15:501–511.
59. Baek JH, Vignesh A, Son H, Lee DH, Roh GS, Kang SS, *et al.* (2019): Glutamine supplementation ameliorates chronic stress-induced reductions in glutamate and glutamine transporters in the mouse prefrontal cortex. Exp Neurobiol 28:270–278.
60. Hasler G, van der Veen JW, Tumonis T, Meyers N, Shen J, Drevets WC (2007): Reduced prefrontal glutamate/glutamine and gamma-aminobutyric acid levels in major depression determined using proton magnetic resonance spectroscopy. Arch Gen Psychiatry 64:193–200.
61. Block W, Träber F, von Widdern O, Metten M, Schild H, Maier W, *et al.* (2009): Proton MR spectroscopy of the hippocampus at 3 T in patients with unipolar major depressive disorder: Correlates and predictors of treatment response. Int J Neuropsychopharmacol 12:415–422.
62. Wagner KV, Hartmann J, Labermaier C, Häusl AS, Zhao G, Harbich D, *et al.* (2015): Homer1/mGluR5 activity moderates vulnerability to chronic social stress. Neuropsychopharmacology 40:1222–1233.
63. Li MX, Li Q, Sun XJ, Luo C, Li Y, Wang YN, *et al.* (2019): Increased Homer1-mGluR5 mediates chronic stress-induced depressive-like behaviors and glutamatergic dysregulation via activation of PERK-eIF2α. Prog Neuropsychopharmacol Biol Psychiatry 95:109682.
64. Fanselow MS, Dong HW (2010): Are the dorsal and ventral hippocampus functionally distinct structures? Neuron 65:7–19.
65. Pilc A, Chaki S, Nowak G, Witkin JM (2008): Mood disorders: Regulation by metabotropic glutamate receptors. Biochem Pharmacol 75:997–1006.
66. Lowery-Gionta EG, Crowley NA, Bukalo O, Silverstein S, Holmes A, Kash TL (2018): Chronic stress dysregulates amygdalar output to the prefrontal cortex. Neuropharmacology 139:68–75.
67. Zhang JY, Liu TH, He Y, Pan HQ, Zhang WH, Yin XP, *et al.* (2019): Chronic stress remodels synapses in an amygdala circuit-specific manner. Biol Psychiatry 85:189–201.
68. DeLorenzo C, Gallezot JD, Gardus J, Yang J, Planeta B, Nabulsi N, *et al.* (2017): In vivo variation in same-day estimates of metabotropic glutamate receptor subtype 5 binding using [^{11}C]ABP688 and [^{18}F]FPEB. J Cereb Blood Flow Metab 37:2716–2727.
69. Elmenhorst D, Mertens K, Kroll T, Oskamp A, Ermert J, Elmenhorst EM, *et al.* (2016): Circadian variation of metabotropic glutamate receptor 5 availability in the rat brain. J Sleep Res 25:754–761.
70. Cyranowski JM, Frank E, Young E, Shear MK (2000): Adolescent onset of the gender difference in lifetime rates of major depression: A theoretical model. Arch Gen Psychiatry 57:21–27.
71. Albert PR (2015): Why is depression more prevalent in women? J Psychiatry Neurosci 40:219–221.